Spectroscopy. X-band CW EPR experiments were performed on a E-90 Varian spectrometer. Pulsed X-band EPR and ENDOR spectra were recorded with a homebuilt spectrometer (at ETH Zürich)[47] equipped with a bridged loop-gap resonator.[48] In the pulsed ENDOR experiments, the microwave (mw) resonator is surrounded by a solenoidal radio frequency (rf) coil that generates the rf field and serves as a mw radiation shield.[49]

The pulse scheme used in the ENDOR experiments[19] consists of the stimulated electron spin–echo sequence, $\pi/2 - \tau - \pi/2 - T - \pi/2 - \tau -$ echo, with nonselective mw pulses and a selective rf pulse of variable frequency ν_{rf} and flip angle $\beta_{rf} = \pi$ applied between the second and third mw pulses (Mims–ENDOR). The following parameters were used: length of the mw $\pi/2$ pulses, $t_{\pi/2} = 30$ ns; length of the rf π pulse, $t_{rf} = 40$ μs; rf increment, $\Delta\nu_{rf} = 10$ kHz; time between the first and second mw pulse, $\tau = 500$ ns ($g_\parallel$) and $\tau = 800$ ns ($g_\perp$); pulse repetition rate, 500 Hz.

In the electron spin–echo envelope modulation (ESEEM) experiments, both the two-pulse sequence, $\pi/2 - \tau - \pi - \tau -$ echo, and the three-pulse sequence, $\pi/2 - \tau - \pi/2 - T - \pi/2 - \tau -$ echo, with pulse lengths $t_{\pi/2} = 10$ ns and $t_\pi = 20$ ns were used. The time (τ in the two-pulse, T in the three-pulse experiment) was increased in increments of $\Delta t = 10$ ns, and time τ in the three-pulse ESEEM was fixed to 200–300 ns. ENDOR and ESEEM signals were recorded at temperatures between 10 and 20 K using a helium gas cooling system. Note that resonators with slightly different resonance frequencies have been used for the different experiments; the nuclear Zeeman frequencies of the ENDOR and ESEEM spectra may therefore not be determined from the EPR spectrum shown in Figure 4.

For the ENDOR measurements, deoxygenated toluene or toluene-d_8 solutions containing **1** (0.02 M) and α-^{13}C-benzaldehyde (99.6 atom % ^{13}C) or benzaldehyde-d_5 respectively (0.1 M; both purchased from Stohler Isotope Chemicals) were used. For the ESEEM studies, deoxygenated toluene solutions containing **1** (0.02 M) and *N*-benzylidene–benzylamine (0.1 M) were prepared.

The zero-frequency component in the time domain ESEEM data was eliminated by subtracting a fitted exponential. For cosine-Fourier transform spectra, the deadtime artifacts were reduced prior to transformation by tapering the ESEEM patterns with a shifted hanning window.

Supplementary Material Available: Tables of bond distances and angles, atomic coordinates, and isotropic thermal parameters; a table collecting bonding parameters for the fragment M–O–C in X-ray characterized complexes containing η^1-coordinated aldehydes, ketones, and esters (including literature references) (7 pages); listings of observed and calculated structure factors (8 pages). Ordering information is given on any current masthead page.

(46) For a selection of compounds containing disordered fluorinated substituents, see, e.g.: (a) Lindoy, L. F.; Lip, H. C.; Louie, H. W.; Drew, M. G. B.; Hudson, M. J. *J. Chem. Soc., Chem. Commun.* **1977**, 778–780. (b) Felthouse, T. R.; Dong, T.-Y.; Hendrickson, D. N.; Shieh, H.-S.; Thompson, M. R. *J. Am. Chem. Soc.* **1986**, *108*, 8201–8214. (c) Kamil, W. A.; Bond, M. R.; Willett, R. D.; Shreeve, J. M. *Inorg. Chem.* **1987**, *26*, 2829–2833. (d) Churchill, M. R.; Fennessey, J. P. *Inorg. Chem.* **1967**, *6*, 1213–1220.

(47) Schweiger, A. In *Modern Pulsed and Continuous Wave Electron Spin Resonance*; Kevan, L., Bowman, M. K., Eds.; Wiley: New York, 1990.

(48) Pfenninger, S.; Forrer, J.; Schweiger, A.; Weiland, T. *Rev. Sci. Instrum.* **1988**, *59*, 752–760.

(49) Forrer, J.; Pfenninger, S.; Eisenegger, J.; Schweiger, A. *Rev. Sci. Instrum.* **1990**, *61*, 3360–3367.

Spectroscopic Detection and Reactivity of the Chlorine Atom–Carbon Disulfide Molecular Complex

John E. Chateauneuf

Contribution from the Radiation Laboratory, University of Notre Dame, Notre Dame, Indiana 46556. *Received June 4, 1992*

Abstract: Pulse radiolysis and laser flash photolysis techniques have been used to generate and kinetically characterize the chlorine atom–carbon disulfide molecular complex ($Cl^\bullet/CS_2$) in CCl_4 solution. The transient absorption spectrum of $Cl^\bullet/CS_2$ has been generated from three independent $Cl^\bullet$ sources: pulse radiolysis of CCl_4, 266-nm photodecomposition of CCl_4, and photodissociation of Cl_2. An absolute rate constant of 1.7×10^{10} M^{-1} s^{-1} for the reaction of $Cl^\bullet + CS_2$ was obtained from both the direct measurement of the decay of the charge-transfer band of $Cl^\bullet$ in CCl_4 ($\lambda_{max} = 330$ nm) and from the formation kinetics of $Cl^\bullet/CS_2$ ($\lambda_{max} = 370$ nm; shoulder = 490 nm). The properties of $Cl^\bullet/CS_2$ are compared with those of the molecular complexes of $Cl^\bullet$ with benzene and pyridine. The reactivity observed monitoring the $Cl^\bullet/CS_2$ absorption band toward 2,3-dimethylbutane has also been investigated to determine the equilibrium constant (K) of the $Cl^\bullet/CS_2$ complex, and the value of K is compared to that determined by direct spectroscopic method. K for the $Cl^\bullet$/pyridine complex has also been reevaluated.

Introduction

Recently, the gas-phase reaction of chlorine atom with carbon disulfide has received considerable attention[1-3] due to its potential importance in atmospheric chemistry. Both the relative rate technique[1,2] and time-resolved fluorescence[3] of chlorine atom have been used to determine that chlorine atom forms a reversible adduct with carbon disulfide.

The importance of the interaction of chlorine atom with carbon disulfide in liquid-phase photochlorination reactions was first reported by Russell.[4-6] Dramatic increases in selectivity in tertiary to primary hydrogen-atom abstractions were observed in the photochlorination of 2,3-dimethylbutane (DMB) in the presence of carbon disulfide[7] or benzene.

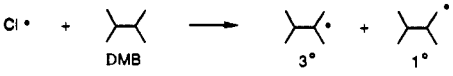

(1)

In the latter case, it is now generally believed that the enhanced tertiary to primary selectivity is a direct consequence of a rapidly formed chlorine atom–benzene π-molecular complex[8,9] (**1**). The

(1) Martin, D.; Barnes, I.; Becker, K. H. *Chem. Phys. Lett.* **1987**, *140*, 195–199.

(2) Wallington, T. J.; Andino, J. M.; Potts, A. R. *Chem. Phys. Lett.* **1991**, *176*, 103–108.

(3) Nicovich, J. M.; Shackelford, C. J.; Wine, P. H. *J. Phys. Chem.* **1990**, *94*, 2896–2903.

(4) Russell, G. A. *J. Am. Chem. Soc.* **1957**, *79*, 2977–2978.

(5) Russell, G. A. *J. Am. Chem. Soc.* **1958**, *80*, 4987–4996.

(6) Russell, G. A. *J. Am. Chem. Soc.* **1958**, *80*, 4997–5001.

(7) Also see: Skell, P. S.; Baxter, H. N.; Taylor, C. K. *J. Am. Chem. Soc.* **1983**, *105*, 120–121.

0002-7863/93/1515-1915$04.00/0

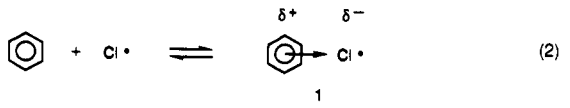

(2)

1

electronic absorption spectrum of the chlorine atom–benzene π-complex was first detected by Bühler[10] upon pulse radiolysis of carbon tetrachloride containing benzene. Subsequently, the reactivity of the chlorine atom–benzene π-complex has been thoroughly investigated by both classical and laser flash photolysis techniques.[7,8,11-13] The molecular complexes of chlorine atom with pyridine[14] and DMSO[15-19] have also been observed with time-resolved spectroscopies; however, the interaction of chlorine atoms with carbon disulfide in solution has not been investigated by direct methods to date.

Herein, the absolute kinetics for the reaction of chlorine atom with carbon disulfide and the spectroscopic detection and reactivity of the $Cl^{\bullet}/CS_2$ complex are presented. Chlorine atom was generated by three independent methods: 355-nm laser photodissociation of molecular chlorine, 266-nm laser photodecomposition of CCl_4, and pulse radiolysis of CCl_4. Absolute kinetics were obtained by time-resolved UV–visible absorption. Spectral and kinetic characteristics of the $Cl^{\bullet}/CS_2$ complex are compared with those of the $Cl^{\bullet}$/benzene and $Cl^{\bullet}$/pyridine complexes.

Experimental Section

Materials. Carbon tetrachloride (Fisher Spectranalyzed) was passed through neutral, activated (Brockmann 1) aluminum oxide (Aldrich) and distilled from K_2CO_3 (35-cm Vigreux column) prior to use. Carbon disulfide (Aldrich, HPLC grade), 2,3-dimethylbutane (Aldrich), benzene (Fisher Spectranalyzed), pyridine (Fisher), cyclohexane (Fisher), and cyclohexyl chloride (Aldrich) were all distilled prior to use. Benzene was washed with concentrated H_2SO_4, saturated $NaHCO_3$, and distilled H_2O and dried over CaH_2 prior to distillation. High-purity molecular chloride (Matheson) was used as received.

Pulse Radiolysis. The pulse radiolysis experiments were performed using a 10-ns pulse of 8-MeV electrons from the Notre Dame Radiation Laboratory linear accelerator. The LINAC pulse radiolysis apparatus has previously been described in detail.[20] The doses used were ~500 rd/pulse as determined by thiocyanate dosimetry. Solutions were flowed through a 1-cm optical path length cylindrical Suprasil cell at a rate of 3–5 mL/min from a solution reservoir connected by either glass or BEV-A-LINE (Cole–Parmer) tubing. Unless stated otherwise, solutions were deoxygenated by bubbling with high-purity nitrogen continuously throughout the experiment.

Laser Flash Photolysis. The LFP apparatus has also been described.[21] Briefly, the third and fourth harmonic of a Quanta Ray DCR-1 Nd:YAG (pulse width ~6 ns) was used for 355- and 266-nm laser excitation, respectively. A pulse 1000-W xenon lamp was used as the monitoring source and signals were digitized with a Tektronix 7912 AD. Experimental control and computer analysis were done using a VAX-11/780. The 266-nm photodecomposition of CCl_4 experiments was performed using focused perpendicular laser excitation (≈9 mJ/pulse) into 9 × 6 mm^2 Suprasil quartz cells. Kinetic experiments were carried out using individually prepared static cells containing 2 mL of either N_2-, air-, or O_2-saturated solution for each concentration of substrate used. Typically 8–10 laser shots were averaged for each kinetic trace. Transient spectra were taken using a flow-cell apparatus. The 355-nm experiments were performed using the same geometrical arrangement with slightly attenuated excitation and ≈8 mJ/pulse. Samples were prepared with presaturated CCl_4 with concentrations of Cl_2 adjusted to 0.6–0.8 OD at 355 nm and then jacketed with the appropriate atmosphere. Typically only one laser shot was required for each kinetic trace.

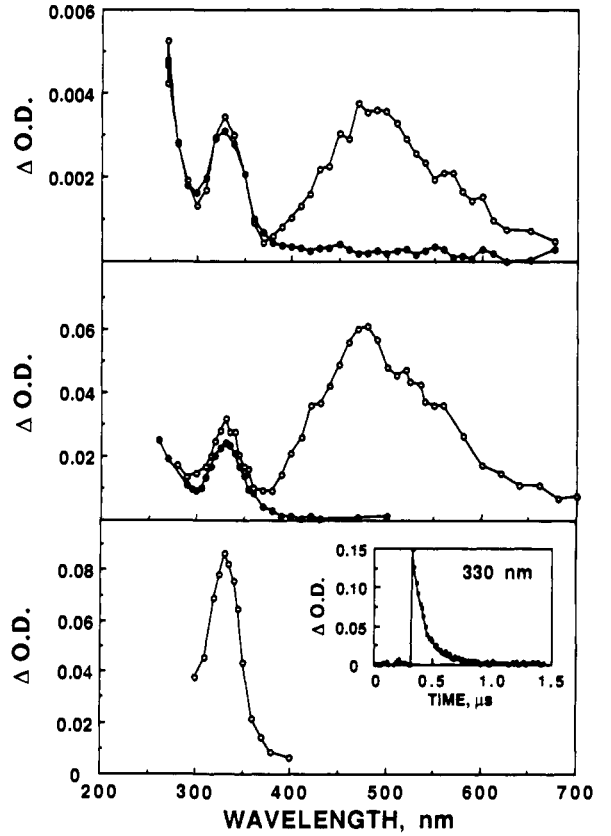

Figure 1. UV–visible absorption spectra observed: (top) 20 ns (○) and 250 ns (●) following pulse radiolysis of CCl_4; (middle) 15 ns (○) and 100 ns (●) following 266-nm LFP of CCl_4; and (bottom) 100 ns (○) following 355-nm LFP of Cl_2 in CCl_4. Insert: typical decay observed at 330 nm.

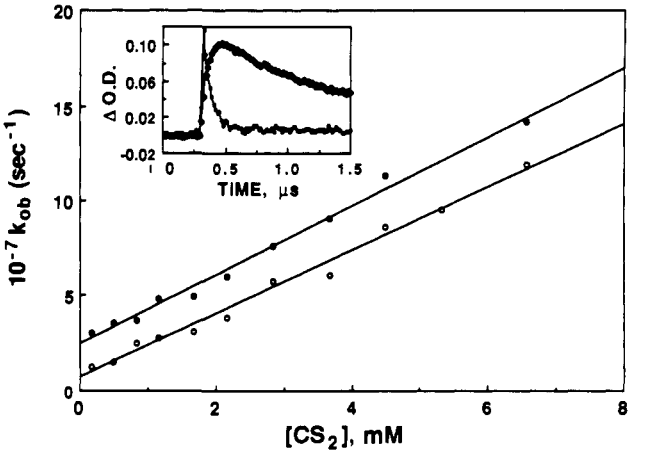

Figure 2. Dependence of the 330-nm decay (○) and 370-nm growth (●) signals (insert) on CS_2 concentration observed following 355-nm LFP of Cl_2 in CCl_4.

(8) See discussions in: (a) March, J. *Advanced Organic Chemistry*, 4th ed.; Wiley-Interscience: New York, 1992; pp 688–689. (b) Reichardt, C. *Solvents and Solvent Effects in Organic Chemistry*, 2nd ed.; VCH Verlagsgesellschaft: Weinheim, 1988; pp 181–183. (c) Ingold, K. U.; Lusztyk, J.; Raner, K. D. *Acc. Chem. Res.* **1990**, *23*, 219–225.

(9) A long-standing proposal suggests that chlorocyclohexadienyl radical is also involved in the photochlorination selectivities.[7] And, while it is also conceivable that the species observed by optical spectroscopy is not that responsible for the observed chlorination selectivities, until definitive experimental evidence is presented supporting this proposal, this author will invoke the more commonly referenced mechanisms, i.e., the π-molecular complex.[8a-c]

(10) Bühler, R. E.; Ebert, M. *Nature* **1967**, *214*, 1220–1221. Bühler, R. E. *Helv. Chim. Acta* **1968**, *51*, 1558–1571.

(11) Bunce, N. J.; Ingold, K. U.; Landers, J. P.; Lusztyk, J.; Scaiano, J. C. *J. Am. Chem. Soc.* **1985**, *107*, 5464–5472.

(12) Raner, K. D.; Lusztyk, J.; Ingold, K. U. *J. Am. Chem. Soc.* **1989**, *111*, 3652–3658.

(13) Raner, K. D.; Lusztyk, J.; Ingold, K. U. *J. Phys. Chem.* **1989**, *93*, 564–570.

(14) Breslow, R.; Brandl, M.; Hunger, J.; Turro, N.; Cassidy, K.; Krogh-Jespersen, K.; Westbrook, J. D. *J. Am. Chem. Soc.* **1987**, *109*, 7204–7206.

(15) Sumiyoshi, T.; Katayama, M. *Chem. Lett.* **1987**, 1125–1126.

(16) Sumiyoshi, T.; Miura, K.; Hagiwara, H.; Katayama, M. *Chem. Lett.* **1987**, 1429–1430.

(17) Alfassi, Z. B.; Mosseri, S.; Neta, P. *J. Phys. Chem.* **1989**, *93*, 1380–1385.

(18) Sumiyoshi, T.; Katayama, M. *Bull. Chem. Soc. Jpn.* **1990**, *63*, 1293–1298.

(19) Sumiyoshi, T.; Watanabe, K.; Syogen, S.; Kawasaki, M.; Katayama, M. *Bull. Chem. Soc. Jpn.* **1990**, *63*, 1584–1586.

(20) Janata, E.; Schuler, R. H. *J. Phys. Chem.* **1982**, *86*, 2078-2084.

(21) Nagarajan, V.; Fessenden, R. W. *J. Phys. Chem.* **1985**, *89*, 2330–2335.

Table I. Rate Constants[a] and Conditions for Reactivity toward DMB Obtained by Monitoring Chlorine Atom Molecular Complexes (Cl•/M)

M	[M] (M)	Cl• source[b]	conditions (saturating gas)	k_{DMB} (M^{-1} s^{-1})[c]	ref
CS_2	0.25	Cl_2/CCl_4	N_2	$(2.7 \pm 0.1) \times 10^5$	
CS_2	0.25	Cl_2/CCl_4	air	$(6.2 \pm 0.1) \times 10^6$	
CS_2	0.25	Cl_2/CCl_4	O_2	$(1.7 \pm 0.05) \times 10^7$	
CS_2	0.25	PR/CCl_4	N_2	$(1.7 \pm 0.1) \times 10^7$	
CS_2	0.25	LFP/CCl_4	N_2	$(2.1 \pm 0.04) \times 10^7$	
CS_2	0.25	LFP/CCl_4	air	$(2.1 \pm 0.03) \times 10^7$	
CS_2	0.25	LFP/CCl_4	O_2	$(1.8 \pm 0.1) \times 10^7$	
CS_2	0.025	LFP/CCl_4	air	$(1.1 \pm 0.1) \times 10^7$	
CS_2	0.005	LFP/CCl_4	air	$(5.1 \pm 0.6) \times 10^6$	
pyridine	0.25	Cl_2/CCl_4	air	2.6×10^5	14
pyridine	0.25	PR/CCl_4	N_2	$(3.8 \pm 0.6) \times 10^5$	
pyridine	0.25	Cl_2/CCl_4	air	$(3.8 \pm 0.5) \times 10^5$	
pyridine	0.25	Cl_2/CCl_4	O_2	$(2.9 \pm 0.5) \times 10^5$	
benzene	~10[d]	Bu'OOBu'/HCl	HCl	4.6×10^7	11
benzene	0.25	Cl_2/CCl_4	air	4.4×10^7	14
benzene	0.25	PR/CCl_4	N_2	$(1.6 \pm 0.1) \times 10^8$	
benzene	0.025	LFP/CCl_4	N_2	$(1.7 \pm 0.1) \times 10^8$	
benzene	0.005	LFP/CCl_4	N_2	$(1.9 \pm 0.2) \times 10^8$	
benzene	0.0025	LFP/CCl_4	N_2	$(1.3 \pm 0.2) \times 10^8$	

[a] Rate constants were measured in this work unless otherwise referenced. [b] Cl_2/CCl_4 = 355-nm LFP of Cl_2 in CCl_4; PR/CCl_4 = pulse radiolysis of CCl_4; LFP/CCl_4 = 266 nm LFP of CCl_4. [c] Errors represent $\pm 2\sigma$. [d] Benzene as solvent.

Ground-state UV–vis spectra were taken on a Perkin-Elmer 3840 diode array spectrophotometer using 1-cm Suprasil cuvettes. All experiments were performed at (21 ± 1) °C.

Results

Pulse radiolysis of pure N_2-saturated CCl_4 results in the transient absorption spectra observed in Figure 1 (top). The spectra were taken at 20 and 250 ns following irradiation, demonstrating the independent nature of the two absorption bands (see Discussion). The UV absorption band, λ_{max} = 330 nm, and the broad visible band are also observed at 15 and 100 ns, respectively, upon 266-nm LFP of neat N_2-saturated CCl_4, Figure 1 (middle). Figure 1 (bottom) is the absorption spectrum observed 100 ns following 355-nm photodissociation of Cl_2 in CCl_4. The decay of the 330-nm signal observed in the Cl_2 photolysis, Figure 1 (bottom, insert), rapidly becomes pseudo-first-order with added CS_2 (Figure 2, insert). In the presence of CS_2 a secondary transient absorption (λ_{max} = 370 nm; shoulder = 490 nm) is observed to "grow-in" at the expense of the 330-nm signal (Figure 2, insert). Measuring the dependence of the observed rate constant, k_{ob}, of the 330-nm decay and the 370-nm growth, on CS_2 concentration, 0.2–6.4 mM (Figure 2), gave bimolecular rate constants, k_{bi}, of (1.7 ± 0.1) and (1.8 ± 0.1) × 10^{10} M^{-1} s^{-1}, respectively. k_{bi} were determined according to $k_{ob} = k_0 + k_{bi}[CS_2]$, where k_0 represents the rate constant for all modes of decay of the 330-nm transient in the absence of CS_2. Errors in all k_{bi} reported represent $\pm 2\sigma$.

In the presence of 0.25 M CS_2, Cl_2 photolysis in CCl_4, 266-nm photolysis of CCl_4, and pulse radiolysis of CCl_4 resulted in the transient absorption spectra having λ_{max} = 370 nm, shoulder = 490 nm, Figure 3: A, B, and C, respectively. Each spectrum was taken at ca. 800 ns following the excitation pulse and have been normalized for direct comparison. The time profile (Figure 3, insert) taken at 370 nm from spectrum B, however, is representative of the time profiles observed in each experiment and throughout each spectrum.

The transient decay in Figure 3 became pseudo-first-order with the addition of DMB. Monitoring at 370 nm, the dependence of k_{ob} with added DMB was measured in N_2-, air-, and O_2-saturated CCl_4. Figure 4A demonstrates the results observed in the 355-nm photolysis of Cl_2 in CCl_4 containing 0.25 M CS_2. Rate constants obtained by monitoring the $Cl^•/CS_2$ complex (as well as the Cl•/pyridine and Cl•/benzene complexes) are summarized in Table I. For comparison the results obtained in the pulse radiolysis of N_2-saturated CCl_4 containing 0.25 M CS_2 are also presented in Figure 4A. Figure 4B demonstrates the results observed in the 266-nm photolysis of CCl_4 containing 0.25 M CS_2. DMB rate constants were also determined in air-saturated CCl_4 containing 25 mM and 5 mM CS_2, Table I (vide infra).

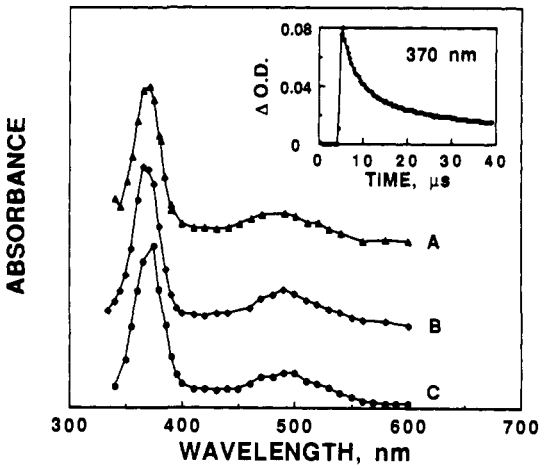

Figure 3. Transient spectra of $Cl^•/CS_2$ observed following: (A) Cl_2 LFP in CCl_4; (B) 266 nm CCl_4 LFP; and (C) pulse radiolysis of CCl_4, each containing 0.25 M CS_2. Insert: decay observed at 370 nm in spectrum B.

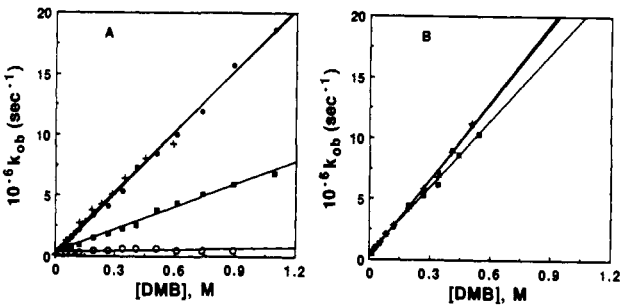

Figure 4. Dependence of k_{ob} measured at 370 nm on DMB concentration in: (A) Cl_2 LFP in (●) O_2-, (■) air-, and (○) N_2-saturated CCl_4 and in the pulse radiolysis (+) of CCl_4 containing 0.25 M CS_2; (B) 266-nm LFP of CCl_4 containing 0.25 M CS_2 in (■) O_2-, (●) air-, and (+) N_2-saturated solutions.

An experiment clearly demonstrating a Cl• radical chain process was also performed. Monitoring 200 ns after 355-nm LFP of 0.7 OD Cl_2 in C_6H_{12} resulted in a spectrum (Figure 5) in which the depletion of Cl_2 and the production of $C_6H_{11}Cl$ is readily observed (vide infra).

The effect of DMB on the Cl•/pyridine complex was reexamined. The Cl•/pyridine complex was generated by both 355-nm LFP of 0.8 OD Cl_2 in CCl_4 containing 0.25 M pyridine and by pulse radiolysis of N_2-saturated CCl_4 containing 0.25 M pyridine.

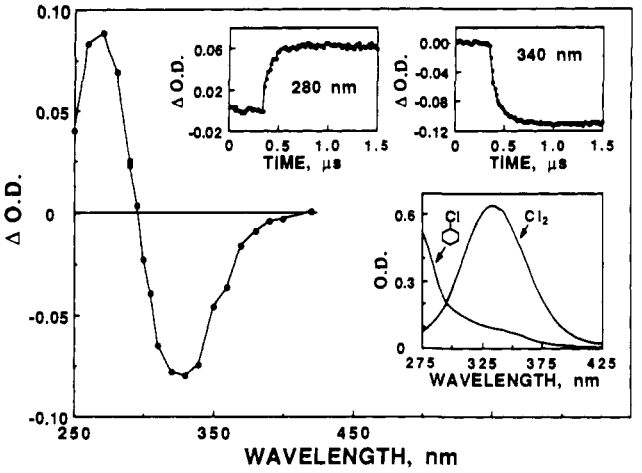

Figure 5. Transient absorption spectrum observed 200 ns following 355-nm LFP of 0.7 OD Cl_2 in cyclohexane. Inserts: (top) time dependence on ΔOD observed at 280 nm and 340 nm; (bottom) ground-state absorption spectra of neat cyclohexyl chloride and Cl_2 in cyclohexane.

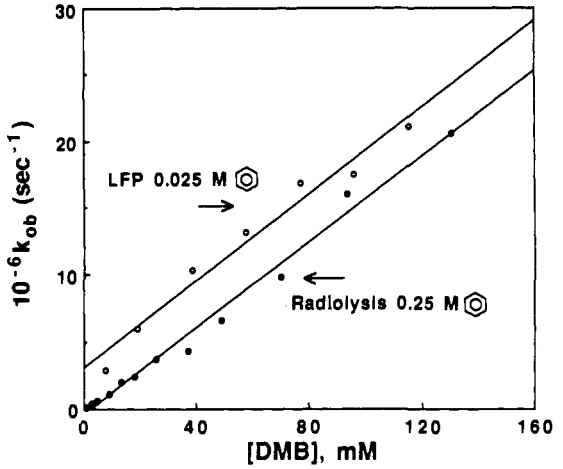

Figure 6. Dependence of k_{ob} on [DMB] for the 310-nm decay observed following: (○) 266-nm LFP of CCl_4 containing 0.025 M benzene; and (●) pulse radiolysis of CCl_4 containing 0.25 M benzene.

k_{DMB} (Table I) were obtained by monitoring the Cl•/pyridine absorption at 370 nm in the LFP experiments with 15–500 mM DMB in O_2- and air-saturated CCl_4. The pulse radiolysis experiment was done in N_2-saturated CCl_4 and [DMB] = 5–1100 mM.

The effect of DMB on the Cl•/benzene complex[11,12,14] was also reexamined. The Cl•/benzene complex was generated by pulse radiolysis of N_2-saturated CCl_4 containing 0.25 M benzene, and by 266-nm LFP of N_2-saturated CCl_4 containing 0.025 M benzene. Monitoring Cl•/benzene at 310 nm, the dependence on k_{ob} with 0.9–135 mM DMB in the pulse radiolysis experiment, and with 7.7–114 mM DMB in the LFP experiment, is presented in Figure 6 and Table I. DMB rate constants were also obtained in 266-nm LFP experiments containing 5 and 2.5 mM benzene (Table I).

Discussion

Generation of Chlorine Atom. Pulse Radiolysis of CCl_4. There is no doubt that pulse radiolysis of CCl_4 is an excellent source of Cl•, as demonstrated by Bühler[10] in the ready detection of the Cl•/benzene π-complex. In fact, yields of Cl• as high as 8.3 atoms/100 eV have been reported in the pulse radiolysis of pure CCl_4.[22] There has, however, been several assignments[23] of the two major absorption bands observed in the pulse radiolysis of CCl_4 (Figure 1, top), and therefore the radiolysis of CCl_4 will be discussed in some detail.

In a simplified scheme, the radiolysis of CCl_4 can be seen to occur by three major pathways. Initial ionization of solvent results in the ejection of an electron, and the solvent derived radical cation:

$$CCl_4 \rightsquigarrow CCl_4^{\bullet+} + e^- \quad (3)$$

The ejected electron is rapidly captured by dissociative electron attachment to solvent

$$e^- + CCl_4 \rightarrow CCl_4^{\bullet-} \rightarrow CCl_3^{\bullet} + Cl^- \quad (4)$$

and the solvent derived radical cation undergoes rapid fragmentation.

$$CCl_4^{\bullet+} \rightarrow CCl_3^{+} + Cl^{\bullet} \quad (5)$$

It is now generally believed[23] that the visible band observed upon pulse radiolysis of CCl_4 is due to some form of CCl_3^+, most likely associated with Cl^-. Unfortunately, far less activity has been devoted to the identification of the 330-nm band. The two most prevalent assignments in the literature[23] are to $CCl_4^{\bullet+}$ and $:CCl_2$ (dichlorocarbene). The assignment to $CCl_4^{\bullet+}$ has been suspect, however, considering $CCl_4^{\bullet+}$ is predicted to be extremely unstable and possess a subnanosecond lifetime.[23b] Recently, $CCl_4^{\bullet+}$ was reported to decay within 100 ps as determined by picosecond pulse radiolysis.[24] The assignment of the 330-nm band to $:CCl_2$, generated from an highly excited state of CCl_4 (eq 6),

$$CCl_4 \rightsquigarrow CCl_4^{**} \rightarrow :CCl_2 + 2Cl^{\bullet} \text{ or } Cl_2 \quad (6)$$

was first proposed by Bühler.[25] It should be noted that this assignment has always been tentative.[23b] This assignment has, however, unfortunately propagated through the literature[23a,24] without experimental support.

***266-nm* Photolysis of CCl_4 and Photodissociation of Cl_2.** Mataga and co-workers[26] demonstrated that picosecond 266-nm multiphoton LFP of CCl_4 also results in the visible absorption band observed in the radiolysis of CCl_4. Washio et al.[27] first indicated that both the UV and visible bands were generated upon 266-nm nanosecond LFP of CCl_4. Again the 330-nm band was attributed to $:CCl_2$.

More recently, it has been demonstrated[28] that the 330-nm band observed upon pulse radiolysis and 266-nm LFP of CCl_4 are spectrally and kinetically identical. For example, rate constants for the reaction of the 330-nm transient with cyclopentene of 1.0 and 1.1×10^{10} M^{-1} s^{-1} were obtained from pulse radiolysis and 266-nm LFP, respectively. It was also demonstrated[28] that 355-nm photodissociation of Cl_2 in CCl_4 (eq 7) generated the 330-nm band

$$Cl_2 \xrightarrow{h\nu} 2Cl^{\bullet} \xrightarrow[CCl_4]{} 2\overset{\delta+}{C}Cl_4 \xrightarrow[330\ nm]{} \overset{\delta-}{Cl}^{\bullet} \quad (7)$$

(Figure 1, bottom) and that *this transient species is kinetically identical with those generated via radiolysis and 266-nm LFP.* Further investigations of reaction 7 in several halogenated solvents has resulted in the identification and assignment of the 330-nm band observed in CCl_4 to a 1:1 solvent charge-transfer (CT) transition of chlorine atom.[29]

Finally, the assignment of the 330-nm band to $:CCl_2$ may fully be dismissed by comparison of the reactivity of the 330-nm transient with both the previously known relative rate data[30] and the recently obtained absolute kinetics[31] of $:CCl_2$ in solution.

(22) Bibler, N. E. *J. Phys. Chem.* **1971**, *75*, 25–30.
(23) For summaries of published assignments, see: (a) Emmi, S. S.; Beggiato, G.; Casalbore-Miceli, G. *Radiat. Phys. Chem.* **1989**, *33*, 29–37. (b) Bühler, R. E. *Radiat. Phys. Chem.* **1983**, *21*, 139–146.
(24) Washio, M.; Yoshida, Y.; Hayashi, N.; Kobayashi, H.; Tagawa, S.; Tabata, Y. *Radiat. Phys. Chem.* **1989**, *34*, 115–120.
(25) Ha, T.-K.; Gremlich, H. U.; Bühler, R. E. *Chem. Phys. Lett.* **1985**, *65*, 16–18.
(26) Miyasaka, H.; Masuhara, H.; Mataga, N. *Chem. Phys. Lett.* **1979**, *118*, 459–463.
(27) Washio, M.; Tagawa, S.; Tabata, Y. *Radiat. Phys. Chem.* **1983**, *21*, 239–243.
(28) Chateauneuf, J. E. *J. Am. Chem. Soc.* **1990**, *112*, 442–444.
(29) Chateauneuf, J. E. *Chem. Phys. Lett.* **1989**, *164*, 577–580.
(30) See: Moss, R. A. *Acc. Chem. Res.* **1980**, *13*, 58–64. Moss, R. A. *Acc. Chem. Res.* **1989**, *22*, 15–21.
(31) Chateauneuf, J. E.; Johnson, R. P.; Kirchhoff, M. M. *J. Am. Chem. Soc.* **1990**, *112*, 3217–3218.

Reaction of Cl• with CS_2. Identification of the CT absorption band of Cl• in CCl_4 (λ_{max} = 330 nm) now allows for the direct measurement of Cl• reactivity from three relatively "clean" independent sources. Even though each source has some experimental limitations (vide infra), a combination of the three allows for a comprehensive understanding of Cl• reactivity in solution.

Bimolecular rate constants of Cl• may be accurately measured under appropriate conditions. These conditions specifically require *no* regeneration of Cl• due to chain processes (see discussion below) and "clean" reagents. The lifetime ($1/k_{ob}$) of Cl• is crucially dependent on CCl_4 purity due to the high and indiscriminate reactivity of Cl•. Therefore, it is necessary to rigorously purify CCl_4 as well as quenching substrates, prior to use (see Experimental Section) in order to observe Cl• in the nanosecond time regime and to extend the dynamic range in which Cl• kinetics may be obtained.

The reactivity of Cl• toward CS_2 could be monitored at 330 nm at low CS_2 concentrations following 355-nm photolysis of 0.6 OD Cl_2 in CCl_4. Congruent growth of the reaction product at 370 nm (Figure 2, insert) could also be used to "probe" Cl• kinetics. Inconsequentially, the absolute values of k measured at 370 nm are slightly larger than those measured at 330 nm (Figure 2) due to spectral overlap with the CT Cl• band. The bimolecular rate constants obtained 1.7 and 1.8 × 10^{10} M^{-1} s^{-1}, are identical within experimental error. A similar experiment was performed following 266-nm LFP of CCl_4 containing 0.5–4.5 mM CS_2 yielding bimolecular rate constants of (2.1 ± 0.1) and (2.9 ± 0.2) × 10^{10} M^{-1} s^{-1} when observed at 330 and 370 nm, respectively. The absolute kinetics measured are assigned to the formation of the Cl•/CS_2 molecular complex (eq 8).

$$Cl^{\bullet} + CS_2 \rightleftharpoons CS_2^{\delta+} \rightarrow Cl^{\bullet\delta-} \qquad (8)$$

The UV–visible absorption spectrum of Cl•/CS_2 is observed (Figure 3) following generation of Cl• from each source described above in the presence of 0.25 M CS_2. Under these conditions the complex is formed within the excitation pulse and possesses a multi-microsecond lifetime (Figure 3, insert). This transient complex is assigned to the species responsible for the enhanced tertiary/primary selectivity reported to range from 33[5,8b] to 107[7] in the photochlorination of DMB in the presence of CS_2.

Apparent Cl•/CS_2 Reactivity toward DMB. Cl_2 Photolysis and the Radical Chain Process. In hopes of further characterizing the Cl•/CS_2 complex, the kinetics of the Cl•/CS_2 absorption[32] toward DMB has been investigated. A strong dependence on O_2 concentration was observed on rate constants obtained by monitoring Cl•/CS_2 at 370 nm in the Cl_2 photolysis in a 0.25 M CS_2/CCl_4 solution with added DMB (Figure 4A). The apparent rate constant in N_2-saturated solution was 2.7 × 10^5 M^{-1} s^{-1}, whereas, rate constants of 6.2 × 10^6 M^{-1} s^{-1} and 1.7 × 10^7 M^{-1} s^{-1} were obtained in solutions containing air and O_2, respectively. A similar O_2 dependence has also been observed[11,12] with the Cl•/benzene π-complex and is attributed to replenishing Cl• within the decay time of the complex through a radical chain process. Clear evidence of Cl• regeneration is observed in the N_2-saturated plot (Figure 4A) where, at high [DMB] k appears to decrease. In fact, a small end of trace "bleach", i.e., negative ΔOD, is observed in the decay traces at these concentrations (vide infra).

A dramatic demonstration of the radical chain process can be seen in the photolysis of Cl_2 in neat cyclohexane. LFP of Cl_2 in deaerated cyclohexane results in an irreversible "bleach" when monitoring within the ground-state absorption band of Cl_2 (λ_{max} = 340 nm) (Figure 5). The bleach *appears* to occur with simple first-order kinetics[33] (Figure 5, insert) at 340 nm. Monitoring at 280 nm, an absorption signal is observed to "grow in" with kinetics similar to the 340-nm bleach. A comparison of the ground-state absorption spectra (Figure 5, insert) with the spectrum observed following LFP (Figure 5) demonstrates that the "bleach" coincides with depletion of Cl_2, and the growth with the radical chain product, cyclohexyl chloride, according to Scheme I. LFP in the presence of O_2 results in competitive trapping of R• and chain inhibition. This is readily observed in an increase in the rate of growth and rate of bleach at 280 and 340 nm, respectively, and an overall decrease in ΔOD with added O_2. Therefore, when monitoring Cl•/CS_2, the change in k_{DMB} with varying O_2 concentrations is a ramification of the degree of involvement of the radical chain process. The potential for Cl• regeneration is greatest at high concentrations of DMB (and Cl_2) and at low concentrations of O_2.

Scheme I

$$Cl_2 \xrightarrow{h\nu} 2Cl^{\bullet}$$
$$Cl^{\bullet} + R\text{–}H \longrightarrow HCl + R^{\bullet}$$
$$R^{\bullet} + Cl_2 \longrightarrow RCl + Cl^{\bullet}$$
$$R^{\bullet} + O_2 \longrightarrow RO_2^{\bullet}$$

Scheme II

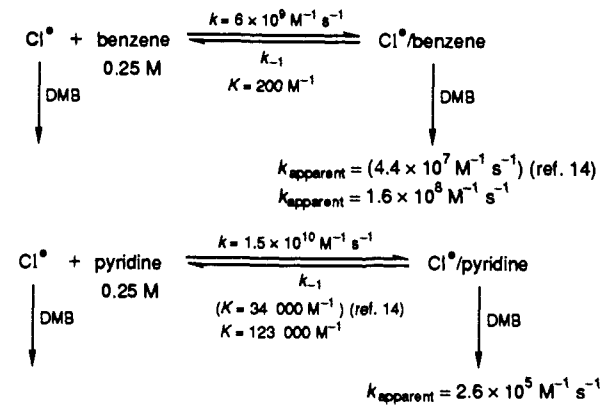

Pulse Radiolysis and 266-nm LFP. Upon completion of the primary processes in the pulse radiolysis of CCl_4, there is virtually no chance of Cl• regeneration, and a k_{DMB} of 1.7 × 10^7 M^{-1} s^{-1} was obtained monitoring the Cl•/CS_2 absorption in N_2-saturated CCl_4. Similar rate constants of 1.8, 2.1, and 2.1 × 10^7 M^{-1} s^{-1} were obtained in O_2-, air-, and N_2-saturated CCl_4 in the 266-nm LFP experiments (Figure 4B). The independence of k_{DMB} on [O_2] indicates there is also no regeneration of Cl• when using this Cl• source. The agreement between the pulse radiolysis and Cl_2 photolysis experiments in O_2-saturated CCl_4 (Figure 4) should also be noted. It is apparent that under the conditions given the [O_2] is sufficiently high that there is little or no contribution of the radical chain process to k_{DMB}. Similar results have been observed with the Cl•/pyridine complex[14] in the presence of O_2 (vide infra).

For direct comparison with the observed Cl•/CS_2 reactivity, the reactivity of "free" Cl• toward DMB has been measured. Pulse radiolysis and 266-nm LFP of CCl_4 resulted in k_{DMB} = (6.8 ± 0.5) and (7.6 ± 0.7) × 10^9 M^{-1} s^{-1}, respectively, when directly monitoring Cl• at 330 nm.

Determination of Equilibrium Constants (K). K of Cl•/Benzene and Cl•/Pyridine. Ingold and co-workers have determined K = 200 M^{-1} for the Cl•/benzene complex. K was obtained from a detailed kinetic analysis of selectivity in the photochlorination of DMB in the presence and absence of benzene. The relative reactivities obtained, and in turn K, were placed on an absolute scale by the LFP determination of k for the reaction of the Cl•/benzene *complex* with DMB in benzene with a nonregenerative Cl• source, and k = 6 × 10^9 M^{-1} s^{-1} for Cl• with benzene.

In their determination of K for the Cl•/pyridine complex, Breslow and co-workers[14] have pointed out that at low concentrations of complexing substrate (e.g., 0.25 M) the transient decay of a fully formed Cl• molecular complex primarily represents the dissociation of the complex to "free" Cl• which is then rapidly

(32) The kinetics measured from the *absorption band* of the Cl• molecular complex toward DMB does not necessarily reflect the reactivity of the complex itself (see discussion on equilibrium constants).

(33) Chain reaction kinetics are, of course, more complicated. See, for example: Espenson, J. H. *Chemical Kinetics and Reaction Mechanisms*; McGraw-Hill: New York, 1981; pp 140–142.

Scheme III

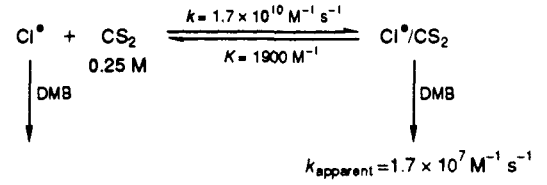

scavenged by DMB. Therefore, having determined a near-diffusion-controlled k for Cl• + pyridine by Stern–Volmer analysis, they obtained $K_{pyridine}$ = 34 000 M^{-1} by $K_{pyridine} = K_{benzene} \times k_{DMB}(benzene)/k_{DMB}(pyridine)$ and Scheme II.

To avoid confusion with k_{DMB} of the *complexes*, $k_{apparent}$ is used in Schemes II and III to denote the rate constants obtained by monitoring the absorption band of the complexes at low concentrations of complexing substrate (vide supra).

Subsequent to the report of Breslow et al.,[14] Raner, Lusztyk, and Ingold[12] indicated that the radical chain process contributes to k_{DMB} when Cl_2 is used as the Cl• source, even in O_2-saturated solution. Therefore, before applying the method described above to determine K for Cl•/CS_2, the Cl•/benzene and Cl•/pyridine systems were reinvestigated.

Agreement in k_{DMB} for Cl•/pyridine determined in 266-nm LFP in O_2- and air-saturated CCl_4 (2.9 and 3.8 × 10^5 M^{-1} s^{-1}) and in pulse radiolysis of N_2-saturated CCl_4 containing 0.25 M pyridine (3.8 × 10^5 M^{-1} s^{-1}) indicated that accurate rate constants could be obtained when Cl_2 was used as the Cl• source in the presence of O_2, as previously described.[14] This was not the case, however, for the Cl•/benzene complex. A k_{DMB} = 4.4 × 10^7 M^{-1} s^{-1} was reported[14] for 355-nm LFP of Cl_2 in CCl_4 containing 0.25 M benzene. In the absence of Cl• regeneration, pulse radiolysis of CCl_4 containing 0.25 M benzene resulted in k_{DMB} = 1.6 × 10^8 M^{-1} s^{-1}, and 266-nm LFP of CCl_4 containing 0.025 M benzene resulted in k_{DMB} = 1.7 × 10^8 M^{-1} s^{-1} (Figure 6). The use of a lower [benzene] in the LFP experiment was due to benzene absorption at the laser wavelength. The relative increase in k_{ob} at lower [benzene] (Figure 6) is a result of a shift in equilibrium to the side of free Cl• in the equation present in the top of Scheme II. Nevertheless, identical k_{bi} for DMB were measured at high and low [benzene], which demonstrated the reactivity observed by monitoring the absorption band of the complex does not, indeed, represent reactivity of the complex itself. For comparison, Ingold et al.[11] have measured k_{DMB} of the *complex* in benzene solution to be k_{DMB} = 4.6 × 10^7 M^{-1} s^{-1}.

The k_{DMB} of the Cl•/benzene absorption band determined by Breslow et al.[14] is nearly an order of magnitude slower than that determined in this work, because of the involvement of the radical chain process. As a result, K for the Cl•/pyridine complex should be reevaluated to K = 123 000 M^{-1}.

K of Cl•/CS_2. The equilibrium constant of the Cl•/CS_2 complex was determined using the above method, as outlined in Scheme III, and the current value of k_{DMB} for Cl•/benzene, which is not contaminated by Cl• regeneration. Accurate values of k_{DMB} for quenching of the Cl•/CS_2 absorption band were obtained in 0.25 M CS_2/CCl_4 solution when pulse radiolysis and 266-nm LFP were used as the Cl• source and in O_2-saturated CCl_4 when Cl_2 was used as the Cl• precursor (Figure 4). Again similar values of k_{DMB} were obtained when lower [CS_2], e.g., 5 and 2.5 mM, were used. Therefore, using k_{DMB} = 1.7 × 10^7 M^{-1} s^{-1} results in K = 1900 M^{-1} for the Cl•/CS_2 molecular complex.

Direct Determination of K. Since it is possible to directly monitor the Cl• absorption, kinetic analysis of eq 9 indicates that it should be possible to directly determine K.

$$Cl^\bullet + CS_2 \underset{k_{-1}}{\overset{k_1}{\rightleftharpoons}} Cl^\bullet/CS_2 \qquad (9)$$

The rate of complex formation is represented as:

$$d[Cl^\bullet]/dt = -k_1[Cl^\bullet][CS_2] + k_{-1}[Cl^\bullet/CS_2]$$

However, since the experiment is performed under pseudo-first-order conditions, i.e., [CS_2] ≫ [Cl•], the kinetic scheme may be

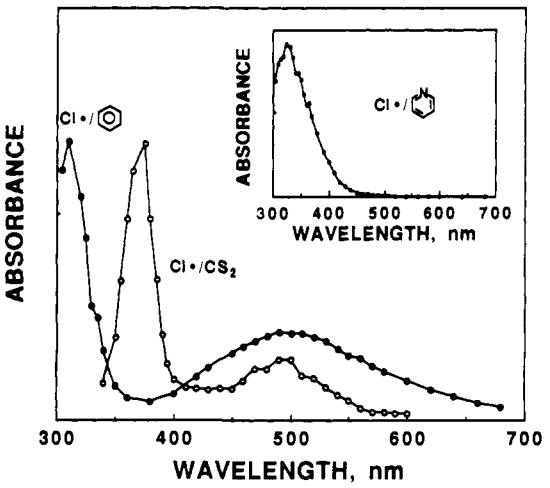

Figure 7. Comparison of normalized spectra of: (●) the Cl•/benzene complex observed 100 ns following 355-nm LFP of Cl_2 in benzene; (○) the Cl•/CS_2 complex as generated in Figure 2c; and the Cl•/pyridine complex (insert) observed 1 μs following 355-nm LFP of 0.8 OD Cl_2 in CCl_4 containing 0.25 M pyridine.

considered as two opposing first-order reactions.[34] k_{ob} is directly obtained by monitoring the ΔOD of Cl• with respect to time ([Cl•] ∝ OD 330 nm) in the presence of CS_2, and

$$k_{ob} = -\frac{d \ln ([Cl^\bullet] - [Cl^\bullet]_\infty)}{dt} = k_1 [CS_2] + k_{-1}$$

Therefore, the quenching plot presented in Figure 2 should yield k_1 as the slope and k_{-1} as the intercept. As a result, K = 1.7 × 10^{10} M^{-1} s^{-1}/7.2 × 10^6 s^{-1} = 2360 M^{-1} which is in excellent agreement with the value obtained in the DMB experiments.

This technique was not applicable to the pyridine complex owing to strong overlap in the absorption band of Cl• with the complex (Figure 7, insert). The technique was attempted, however, with the Cl•/benzene complex by measuring the growth of the complex at 490 nm[35] following 355-nm LFP of Cl_2 in CCl_4 containing 1.7–11.2 mM benzene. It should be noted that measuring growth kinetics in this dynamic range is not very reliable; nevertheless, the resultant quenching plot yielded K = (1.3 ± 0.2) × 10^{10} M^{-1} s^{-1}/(6.9 ± 0.2) × 10^7 s^{-1} = 188 M^{-1}.

Comparison of Cl• Complexes. The degree of interaction of Cl• with benzene, CS_2, and pyridine can readily be seen in the tertiary/primary selectivity observed in the photochlorination of DMB.[7,14] In the presence of 4 M complexing agent and at low [DMB] (<0.1 M), tertiary/primary ratios are reported to be ca. 50/1, 100/1, and 200/1 for the benzene,[7] CS_2,[7] and pyridine[14] complexes, respectively.

The reactivity observed for the Cl•/benzene complex is generally believed to reflect that of a π-molecular complex.[8] A combination of selectivity, LFP, and computational results led Breslow et al.[14] to assign to Cl•/pyridine complex to a N–Cl σ-type adduct. This assignment has recently been verified from the matrix isolation EPR spectrum of the three-electron-bond intermediate.[36] The Cl•/CS_2 complex has also been described as a σ-type complex[8b] which would be formed by Cl• attack on CS_2 carbon, as represented in eq 10.

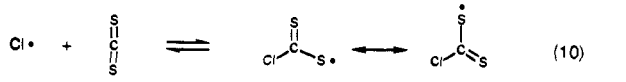

(10)

A recent computational study[37] (Hartree–Fock 3-21G(*) level) has derived a similar C_s structure having one C—S and one C=S bond; however, a C_{2v} structure possessing distances intermediate

(34) See ref. 33, pp 45–48.
(35) The UV band of Cl•/benzene could not be used for this purpose owing to overlap with the Cl•/CCl_4 CT band.
(36) Abu-Raqabah, A.; Symons, M. C. R. *J. Am. Chem. Soc.* **1990**, *112*, 8614–8615.
(37) Marshall, P. THEOCHEM **1991**, *82*, 309–319.

between typical C-S single and double bonds was also suggested. In addition it was reported that no evidence was found for Cl• bonding at alternative sites.

It is beyond the scope of this investigation to determine the structural nature of the $Cl^•/CS_2$ complex. It is, however, interesting to compare the UV-visible absorption spectra of the Cl• benzene, CS_2, and pyridine complexes (Figure 7) and note the dramatic resemblance of the $Cl^•/CS_2$ spectrum to that of the π-benzene complex. The equilibrium constants determined in this work[38] do confirm the strength of interaction of Cl• with CS_2 to be intermediate between the π-benzene and σ-pyridine complexes, i.e., 200 M^{-1} > 1900 M^{-1} > 123 000 M^{-1}.

(38) It should be noted that considerable error may still be associated with the absolute values of K determined by comparison with the 200 M^{-1} value for Cl•/benzene if k_{bi} for Cl• + benzene determined in this work represents a more accurate measurement.

Conclusions

The reactivity of Cl• toward CS_2 to form a reversible $Cl^•/CS_2$ molecular complex has been investigated by time-resolved pulse radiolysis and LFP techniques. The equilibrium constant of the $Cl^•/CS_2$ complex has been determined and is compared to that of the Cl•/benzene π-complex and a reevaluated K for the Cl•/pyridine σ-complex.

Acknowledgment. The work described herein was supported by the Office of Basic Energy Sciences of the Department of Energy. This is Contribution No. NDRL-3502 from the Notre Dame Radiation Laboratory.

Determination of Metal-Hydride and Metal-Ligand (L = CO, N_2) Bond Energies Using Photoacoustic Calorimetry†

Simon T. Belt, J. C. Scaiano,* and Michael K. Whittlesey

Contribution from the Department of Chemistry, University of Ottawa, Ottawa K1N 6N5, Canada. *Received July 23, 1992*

Abstract: Photoacoustic calorimetry has been used to determine the M-H mean bond dissociation energies in $Ru(dmpe)_2H_2$ (dmpe = $Me_2PCH_2CH_2PMe_2$) and $H_2IrCl(CO)(PPh_3)_2$ (63.5 ± 2.0 and 64.0 ± 1.0 kcal mol^{-1}, respectively). The quantum yield for loss of H_2 from the ruthenium dihydride complex has been measured by transient actinometry as 0.85 ± 0.05. $Ru(dmpe)_2$ is an unsolvated intermediate and reacts with CO and N_2 to form $Ru(dmpe)_2CO$ and $Ru(dmpe)_2N_2$. By measuring the enthalpies of these reactions and utilizing the Ru-H mean bond dissociation energy, the Ru-CO and Ru-N_2 bond energies have been determined (43.0 ± 2.0 and 18.8 ± 2.0 kcal mol^{-1}, respectively).

Introduction

Transition metal hydride complexes represent an important class of organometallic compounds because of their ability to function in a variety of catalytic and stoichiometric processes.[1] For such processes to be considered in any detail, a knowledge of both kinetic and thermodynamic factors is desirable. Although kinetic studies regarding metal hydride forming/breaking processes have received constant attention,[2] there is a notable paucity of accurate values for M-H bond enthalpies in the literature, a fact which arises from the difficulty in making such measurements.[3] Isolated examples have employed kinetic measurements,[4] conventional solution calorimetry,[5] and, more recently, electrochemical cycles.[6]

Photoacoustic calorimetry (PAC) has received considerable attention and has been used to examine the energetics of a host of biochemical, organic, and organometallic reactions.[7] The PAC experiment detects, by way of the resulting thermal expansion of the solvent, the heat released into solution from reactions initiated by absorption of a laser pulse. Provided that the mechanism and the quantum yield for the photochemical reaction are well defined, the enthalpy changes due to assigned chemical processes can be evaluated. In many cases, this overall enthalpy change may be attributed to the cleavage and/or formation of specific bonds.

In the field of organometallic photochemistry, studies have concentrated on determining the metal-carbonyl bond energies in the group 6 hexacarbonyl complexes $M(CO)_6$ (M = Cr, Mo, W) and the energetics of the subsequent reaction between $M(CO)_5$ and alkane solvents.[8] The initial photodissociation of CO from $Cr(CO)_6$ and the ensuing solvent coordination to $Cr(CO)_5$ occurs in less than 25 ps.[9] The replacement of CO in $Cr(CO)_6$ by heptane is endothermic by 27 kcal mol^{-1} and yields a value for the chromium-solvent interaction of 9.8 kcal mol^{-1}.[10] In the case of a more coordinating medium (Et_3SiH), the chromium-solvent interaction was measured to be 21 kcal mol^{-1}.[11] Although this solvation effect is itself of primary significance, it is precisely this phenomenon which can be an underlying problem in evaluating not only the absolute bond energies of photolabile ligands, but also the energetics of subsequent reactions between organometallic fragments and an incoming ligand such as H_2 or CO. In this latter

† Dedicated to the memory of Professor Jean-Louis Roustan.

(1) Pearson, R. G. *Chem. Rev.* **1985**, *85*, 41.
(2) Geoffroy, G. L.; Wrighton, M. S. *Organometallic Photochemistry*; Academic Press: New York, 1979.
(3) Martinho Simoes, J. A.; Beauchamp, J. L. *Chem. Rev.* **1990**, *90*, 629.
(4) Vaska, L.; Werneke, M. F. *Trans. N.Y. Acad. Sci., Ser. 2* **1971**, *33*, 70.
(5) (a) Landrum, J. T.; Hoff, C. D. *J. Organomet. Chem.* **1985**, *282*, 215. (b) Connor, J. A.; Zafarani-Moattar, M. T.; Bickerton, J.; El Saied, N. I.; Suradi, S.; Carson, R.; El Takhin, G.; Skinner, H. A. *Organometallics* **1982**, *1*, 1166.
(6) Tilset, M.; Parker, V. D. *J. Am. Chem. Soc.* **1989**, *111*, 6711.
(7) (a) Heihoff, K.; Braslavsky, S. E.; Schaffner, K. *Biochemistry* **1986**, *26*, 6803. (b) Peters, K. S.; Watson, T.; Logan, T. *J. Am. Chem. Soc.* **1992**, *114*, 4276. (c) Rudzki, J. E.; Goodman, J. L.; Peters, K. S. *J. Am. Chem. Soc.* **1985**, *107*, 7849. (d) Burkey, T. J.; Majewski, M.; Griller, D. *J. Am. Chem. Soc.* **1986**, *108*, 2218. (e) Griller, D.; Wayner, D. D. M. *Pure Appl. Chem.* **1989**, *61*, 717. (f) Ni, T.; Caldwell, R. A.; Melton, L. A. *J. Am. Chem. Soc.* **1989**, *111*, 457. (g) Yang, G. K.; Peters, K. S.; Vaida, V. *Chem. Phys. Lett.* **1986**, *125*, 566. (h) Herman, M. S.; Goodman, J. L. *J. Am. Chem. Soc.* **1989**, *111*, 9105. (i) Klassen, J. K.; Selke, M.; Sorensen, A. A.; Yang, G. K. *J. Am. Chem. Soc.* **1990**, *112*, 1267.
(8) Yang, G. K.; Vaida, V.; Peters, K. S. *Polyhedron* **1988**, *27*, 2181.
(9) Simon, J. D.; Peters, K. S. *Chem. Phys. Lett.* **1983**, *98*, 53.
(10) Morse, J., Jr.; Parker, G.; Burkey, T. J. *Organometallics* **1989**, *8*, 2471.
(11) Burkey, T. J. *J. Am. Chem. Soc.* **1990**, *112*, 8329.

0002-7863/93/1515-1921$04.00/0